

Resonant and Nonresonant Multiphoton Ionization Processes in the Mass Spectrometry of Explosives

Hamachi, Akifumi

Department of Applied Chemistry, Graduate School of Engineering, Kyushu University

Okuno, Tomoya

Department of Applied Chemistry, Graduate School of Engineering, Kyushu University

Imasaka, Tomoko

Laboratory of Chemistry, Graduate School of Design, Kyushu University

Kida, Yuichiro

Department of Applied Chemistry, Graduate School of Engineering, Kyushu University

他

<https://hdl.handle.net/2324/7170845>

出版情報 : Analytical chemistry. 87 (5), pp.3027-3031, 2015-03-03. American Chemical Society
バージョン :
権利関係 :



Resonant and Nonresonant Multiphoton Ionization Processes in the Mass Spectrometry of Explosives

**Akifumi Hamachi,[†] Tomoya Okuno,[†] Tomoko Imasaka,[#] Yuichiro Kida,[†]
Totaro Imasaka,^{†, § *}**

*[†]Department of Applied Chemistry, Graduate School of Engineering, Kyushu University,
744 Motoooka, Nishi-ku, Fukuoka 819-0395, Japan*

*[#]Laboratory of Chemistry, Graduate School of Design, Kyushu University, 4-9-1 Shiobaru,
Minami-ku, Fukuoka 815-8540, Japan*

*[§]Division of Optoelectronics and Photonics, Center for Future Chemistry, Kyushu University,
744 Motoooka, Nishi-ku, Fukuoka 819-0395, Japan*

* To whom correspondence should be addressed. E-mail: imasaka@cstf.kyushu-u.ac.jp

ABSTRACT

Multiphoton ionization processes were studied for three types of explosives using a line-tunable ultraviolet femtosecond laser. When peroxides such as triacetone triperoxide (TATP) and hexamethylene triperoxide diamine (HMTD) were ionized through a nonresonant two-photon process, a molecular ion was dominantly observed by reducing the excess energy remaining in the ion. However, an aromatic nitro compound such as 2,4,6-trinitrotoluene (TNT) produced large signals arising from molecular and fragment ions by resonant two-photon ionization. In addition, only fragment ions were produced from a non-aromatic nitro compound such as 1,3,5-trinitroperhydro-1,3,5-triazine (RDX), even when a resonant two-photon ionization process was employed, suggesting that a further reduction in excess energy would be necessary if a molecular ion were to be observed.

A variety of explosives are used in terrorist attacks. Some are peroxides such as triacetone triperoxide (TATP) and hexamethylene triperoxide diamine (HMTD), an aromatic nitro compound of 2,4,6-trinitrotoluene (TNT) and analogs, and thereof non-aromatic nitro compounds, e.g., 1,3,5-trinitroperhydro-1,3,5-triazine (RDX) and pentaerythritol tetranitrate (PETN). Since only a small amount of residues remain at the location of an explosion, it is necessary to use a sensitive analytical instrument for purposes of detection and identification. In addition, to identify the actual criminal, a reliable, highly selective method is needed. Numerous techniques have been developed to date for the measurement of the explosives. For example, Raman spectrometry (RS), ion mobility spectrometry (IMS), liquid chromatography combined with mass spectrometry (LC/MS), and gas chromatography combined with mass spectrometry (GC/MS) can be successfully utilized for this purpose.¹ Among them, it is well known that GC/MS is a sensitive and selective tool for the measurement of various types of explosives. A few types of ionization techniques such as electron ionization and chemical ionization are employed in conjunction with MS. However, a molecular ion is seldom observed in the case of electron ionization, and pseudo molecular ions are inevitably produced in the case of positive/negative chemical ionization. The lack of a molecular ion deteriorates reliability in an analysis, since small molecules whose structures are similar to those of the fragments are frequently present in the environment. On the other hand, the technique of laser ionization (LI) is useful in many cases for observing a molecular ion and is known as a soft ionization method.² Several papers reporting on the measurement of the explosives using GC/LI-MS have appeared.^{3,4,5} The ionization process has, however, not yet been studied in detail.

There are two major types of laser ionization techniques, i.e., single photon ionization (SPI) and multiphoton ionization (MPI). In SPI, the signal intensity gradually increases with an increase in the excess energy above the ionization energy (IE).⁶ Thus, the excess energy cannot be minimized

without detracting from the signal intensity. On the other hand, the ion signal immediately increases above the IE in MPI, then the excess energy can be minimal.⁷ Two types MPI techniques have been reported, i.e., resonance-enhanced (resonant) multiphoton ionization (REMPI) and nonresonant multiphoton ionization (NRMPI). In REMPI, a molecule is excited by absorbing the first photon, the energy of which is optimized for a transition to the singlet excited state. The molecule is, then, ionized by absorbing the second photon during a period of the lifetime of the excited state. In this case, the ionization efficiency is strongly enhanced by the resonance effect.⁸ In NRMPI, a molecule absorbs a few photons simultaneously for the ionization. The efficiency in REMPI is generally higher than that in NRMPI. The efficiency of NRMPI can, however, be improved by an increase in the peak power of the laser. A tunable femtosecond laser would be an attractive ionization source for enhancing efficiency by REMPI and also to reduce the excess energy in NRMPI, thus permitting a molecular ion to be observed.

The IE of explosives are in the order of 8 ~ 11 eV, as calculated in a later section of this paper. A femtosecond laser tunable in the near-infrared (NIR) region can be generated based on optical parametric amplification, the wavelength of which can be extended to the deep-ultraviolet (DUV) region using a technique of harmonic generation followed by sum-frequency mixing in a nonlinear optical crystal. Although such a laser is commercially available, its shorter wavelength is practically limited to 235 nm; the wavelength can be extended to a shorter wavelength, but the system becomes more complicated and the pulse energy decreases substantially. On the other hand, it is possible to generate numerous emission lines from the vacuum-ultraviolet (VUV) to the infrared (IR) region based on four-wave Raman mixing.⁹ Because the laser emissions are generated at the same time, they can be used simultaneously or some of them can be used after beam separation and recombination depending on the specific application.

In this study, we generated a femtosecond laser emitting in the DUV region, i.e., 219, 241, 267

nm, based on four-wave Raman mixing using a vibrational transition of molecular hydrogen for use as an ionization source in GC/MPI-MS. The REMPI and NRMPI processes were studied in detail in an attempt to obtain a molecular ion for explosives such as TATP, HMTD, TNT, RDX, and PETN.

EXPERIMENTAL SECTION

Analytical Instrumentation. A 1- μ L aliquot of a sample solution was injected into a GC system (6890GC, Agilent Technologies, CA) using an auto sampler (7683B, Agilent Technologies). The instrument, a time-of-flight mass spectrometer (TOF-MS), was developed in our laboratory and is commercially available (HGK-1, Hikari-GK, Fukuoka, Japan).¹⁰ The ions, which are accelerated into a flight tube, were detected by an assembly of microchannel plates (MCP, F4655-11, Hamamatsu, Shizuoka, Japan), and the signal was recorded using a digitizer (Acqiris AP240, Agilent Technologies). Details of the experimental apparatus are reported elsewhere.¹¹

Ionization Source. An optical parametric amplifier (OPerA-Solo, <50 fs, Coherent, Inc.) was pumped by a Ti:sapphire laser (Legend-Elite, 802 nm, 1 kHz, 4 mJ, 35 fs, Coherent, Inc.) to generate a NIR femtosecond pulse at 1203 nm. A portion of the remaining output beam of the Ti:sapphire laser was used for the generation of the third harmonic emission (267 nm). As shown in Fig. 1, the other portion of the output beam of the Ti:sapphire laser (802 nm) and the output beam of the optical parametric amplifier (1203 nm) were simultaneously focused into a fused-silica capillary filled with hydrogen gas for molecular phase modulation. The third harmonic emission (267 nm) was then introduced into the capillary after a time delay, the frequency of which was modulated to generate numerous vibrational emissions. The laser emitting at 219, 241, and 267 nm was separated from each other using a series of specially-designed dielectric multilayer mirrors with low dispersions (Sigma Koki Co., Ltd.), and the optical pulse chirped during the transmission of the optics and the ambient air was compressed by dispersion compensation using a pair of prisms. The

pulse energies of the laser were 0.36, 0.64, and 2.5 μJ at 219, 241, and 267 nm, respectively. A detailed description of the system and the performance characteristics will be reported elsewhere.

GC Separation. A DB-5MS column (length 30 m, 0.25 mm inner diameter, 0.25 μm film thickness, Agilent Technologies Inc.) was employed for the separation of the explosives. The temperatures of the GC oven were set at 50 $^{\circ}\text{C}$ (3 min) – 8 $^{\circ}\text{C}/\text{min}$ – 130 $^{\circ}\text{C}$ – 20 $^{\circ}\text{C}/\text{min}$ – 180 $^{\circ}\text{C}$ (5 min) for TATP, 40 $^{\circ}\text{C}$ (3 min) – 10 $^{\circ}\text{C}/\text{min}$ – 160 $^{\circ}\text{C}$ – 25 $^{\circ}\text{C}/\text{min}$ – 230 $^{\circ}\text{C}$ (3 min) for HMTD, 40 $^{\circ}\text{C}$ (5 min) – 10 $^{\circ}\text{C}/\text{min}$ – 280 $^{\circ}\text{C}$ (1 min) for TNT and RDX, and 50 $^{\circ}\text{C}$ (3 min) – 8 $^{\circ}\text{C}/\text{min}$ – 180 $^{\circ}\text{C}$ (5 min) for PETN. Helium was used as the carrier gas, and the flow rate was adjusted at 1.2 mL/min for TATP and 1.0 mL/min for the other explosives. The temperature of the inlet port of GC was maintained at 220 $^{\circ}\text{C}$ for TNT, RDX, and HMTD, and at 110 $^{\circ}\text{C}$ for TATP and PETN.

Sample. Five explosives (Accustandard, Inc.) were used in this study, i.e., TATP (0.1 $\mu\text{g}/\text{mL}$ in acetonitrile), HMTD (0.1 $\mu\text{g}/\text{mL}$ in acetonitrile), TNT (1.0 $\mu\text{g}/\text{mL}$ in a mixture of acetonitrile and methanol (1:1)), RDX (1.0 $\mu\text{g}/\text{mL}$ in a mixture of acetonitrile and methanol (1:1)), and PETN (1.0 $\mu\text{g}/\text{mL}$ in methanol). The internal standard was 3, 4-dinitrotoluene (Tokyo Kasei).

Quantum Chemical Calculation. The UV absorption spectrum and the ionization energy have been calculated and reported for the explosives elsewhere.^{12,13} However, we recalculated the UV absorption spectra in the entire VUV-DUV region and the ionization energy so as to provide more detailed information. The procedure for the calculation was based on the density functional theory (DFT) using the Gaussian09 program and the details were reported elsewhere.¹⁴ The energies were calculated using the B3LYP method at the level of cc-pVDZ.

RESULTS AND DISCUSSION

Figure 2 shows the chromatograms for the explosives. Figure 2 (b) consists of several peaks, which would arise from isomers of HMTD, since the mass spectra measured at these retention times

are the same to each other. A few small peaks in Fig. 2 (c) can be assigned to impurities in the reagent of TNT. Thus, the effect of contamination can be reduced by using GC.

TATP and HMTD. Figure 3 shows the results for TATP, a peroxide explosive. The graph shown in Fig. 3 (a) is the calculated UV absorption spectrum, suggesting that the absorption maximum is located in the VUV region. Although the first electronic excited state is located at an energy corresponding to 224 nm, the oscillator strength is nearly zero. As a result, the favorable effect by REMPI would be negligibly small. The ionization energies calculated for two configurations with D_3 and C_2 symmetries were 8.67 and 8.33 eV, respectively, and the two-photon limits for ionization were calculated to be 4.34 and 4.17 eV, respectively. Accordingly, nonresonant two-photon ionization (NR2PI) would be achieved at all the wavelengths of 267, 241, 219 nm (4.64, 5.15, 5.67 eV). As a result, the excess energy drastically increases at shorter wavelengths. Figure 3 (b) shows a mass spectrum measured at 267 nm. A large signal observed at $m/z = 222$ can be assigned to a molecular ion and a signal at $m/z = 43$ to a fragment ion, $C_2H_3O^+$. The ratio of the intensities of the molecular ion peak and the base peak was 150%. As summarized in Table 1, an ultrashort optical pulse compressed using a pair of prisms appears to be useful for enhancing the intensity of the molecular ion peak. Figures 3 (c) and (d) show results obtained at 241 and 219 nm, respectively. It should be noted that only fragment ions are observed in the mass spectra. The excess energy is zero at 286 and 298 nm for conformers with D_3 and C_2 symmetries, respectively. The calculated excess energy is 0.60 (0.94), 1.63 (1.97), and 2.66 (3.00) eV for TATP with a D_3 (C_2) symmetry at laser wavelengths of 267, 241, and 219 nm, respectively. Accordingly, a large molecular ion was observed at 267 nm and the fragment ions were efficiently produced at 241 and 219 nm due to the large excess energies. Thus, it is important to minimize excess energy to enhance the molecular ion. It has been reported that SPI produces a molecular ion smaller than the fragment ion at 118 nm.⁴ In this case, the excess energy is calculated to 1.83 (2.17) eV, and such a large excess energy would

accelerate the fragmentation. Decreasing the excess energy by changing the wavelength of the VUV light source would be useful in terms of reducing the fragment ions at the expense of the signal intensity. Thus, NR2PI is preferable for suppressing the fragmentation and enhancing the intensity of the molecular ion.

Figure 4 shows the results for HMTD. Similar to TATP, the absorption maximum is located in the VUV region, and the effect of REMPI is negligible in the DUV region due to the near-zero oscillator strengths. Since the ionization energy was calculated to be 8.15 eV, the process would be NR2PI at wavelengths of 219, 241, and 267 nm. Figure 4 (b) shows a mass spectrum measured at 267 nm, in which only a molecular ion is observed. The excess energy at this wavelength was calculated to 1.13 eV, which is slightly larger than the value of 0.60 or 0.94 eV for TATP. This fact suggests that an ionic form of HMTD would have a higher stability. In the case of electron ionization, the intensity of a molecular ion is similar to those of the fragment ions.¹⁷ Thus, the excess energy induced in electron ionization (70 eV) would enhance fragmentation, which is in contrast to soft ionization using a DUV femtosecond laser in the present study. Figures 4 (c) and (d) show mass spectra measured at 241 and 219 nm, respectively. Neither a molecular ion nor a fragment ion was observed. This result would originate from a small absorptivity in the range of two-photon absorption at 110 ~ 121 nm, a larger excess energy, and a low pulse energy available at these wavelengths. As demonstrated herein, a molecular ion can be enhanced for peroxides such as TATP and HMTD by reducing the excess energy in NR2PI.

TNT. Figure 5 (a) shows the calculated UV absorption spectrum for TNT. This compound has a large absorption maximum in the DUV region, since the molecule contains an aromatic ring. This spectral feature is in contrast to peroxides such as TATP and HMTD. Because of this, it would be possible to utilize a REMPI process. The calculated ionization energy was 10.3 eV, suggesting 2PI at 219 and 241 nm and three-photon ionization (3PI) at 267 nm. Figure 5 (b) shows a mass

spectrum measured at 267 nm. The peak at $m/z = 210$ can be assigned to a fragment ion, $[M-17]^+$. It has been reported that an OH group easily dissociates after the rearrangement of the molecular ion.^{18,19} Since TNT is ionized through a 3PI process at 267 nm, the fragmentation would be enhanced by the large excess energy remaining in the ion. Figure 5 (c) shows the result measured at 241 nm, in which a molecular ion was observed in addition to many fragment ions. Figure 5 (d) shows the result obtained at 219 nm, in which the signal-to-noise ratio was drastically improved. This favorable result would appear by RE2PI at 219 nm. Although DFT calculations suggest a RE2PI process at 241 nm, the calculated excess energy was 0.01 eV. Due to an inevitable error in the DFT calculation, the energy required for two-photon ionization in this experiment would be slightly larger than the calculated value. Thus, a molecular ion was observed for TNT, but fragment ions were also produced. A molecular ion could be exclusively observed at a wavelength slightly larger than 219 nm, e.g., at around 230 nm.

The photoionization process for TNT has been studied elsewhere^{3,4, 20,21} and only a molecular ion is observed using SPI with a VUV photon (118 nm). The calculated excess energy was 0.20 eV, resulting in a molecular ion being observed exclusively at this wavelength. On the other hand, numerous fragment ions were observed, in addition to a molecular ion, under MPI at 485, 412, and 325 nm, in which five-, four-, and three-photon ionizations are necessary and the excess energies were calculated to be 2.49, 1.75, and 1.16 eV, respectively. A molecular ion was not observed and only fragment ions were produced when measured at 795 nm. It should be noted that a molecular ion was not observed at 206 nm, which is probably due to the large excess energy in RE2PI. On the other hand, a UV nanosecond laser (267 nm, 5 ns, 800 μ J) was employed for the desorption/ionization of TNT prepared in the form of a pellet, although a molecular ion was not observed.²² An electron ionization source used in the National Institute of Standards and Technology (NIST) database provides no molecular ion in the mass spectrum.²² Accordingly, it

would be important to minimize the excess energy in RE2PI for observing a molecular ion of TNT.

RDX and PETN. Figure 6 (a) shows the calculated UV absorption spectrum of RDX, a non-aromatic ring-containing nitro compound. This molecule has an absorption band in the DUV region and the calculated ionization energy was 10.2 eV, suggesting NR3PI at 267 nm and nearly RE2PI at 241 and 219 nm. The mass spectra measured at 267, 241, and 219 nm are shown in Figs. 6 (b), (c), and (d), respectively. Only fragment ions were observed at these wavelengths, i.e., no molecular ion was observed even at 241 and 219 nm, which is in contrast to TNT. The calculated excess energy was 0.10 and 1.13 eV at 241 and 219 nm, respectively. Resonant two-photon ionization would less likely to occur due to a lower absorptivity than the value for TNT. An NO₂ group in RDX with sufficient excess energy is known to easily dissociate from a molecular ion.²³ It has been reported that a molecular ion is seldom observed for RDX in SPI.⁶ Similar to RDX, an NO₂ group easily dissociates to form fragment ions in the case of 2,3-dimethyl-2,3-dinitrobutane (DMNB) to stabilize the ion.²⁴ As a result, the excess energy should be minimized more carefully to observe a molecular ion for a non-aromatic nitro compound. It is possible that an NO₂ group dissociates automatically to stabilize the ion and that a molecular ion cannot exist in the case of RDX and its analogs.

Figure 7 shows the calculated UV absorption spectrum for PETN, which has an absorption band in the VUV region. The ionization energy was 10.7 eV, which was the largest value among the compounds considered in this study. As a result, NR2PI is possible only at 219 nm. In the experiment, neither a molecular ion nor fragment ions were observed at any wavelength. In a previous study, NO₂⁺ was observed in SPI.⁶ The reason for why no signal was observed in this study could be the low pulse energy of the laser emitting at 219 nm. In order to measure PETN, it would be desirable to use a RE2PI process with a laser emitting at 200 nm or a NR2PI process with a high-peak-power laser emitting at ca. 230 nm, which would reduce the excess energy and possibly

permit a molecular ion to be observed.

CONCLUSIONS

The effect of REMPI and the control of the excess energy represent two major factors that affect the MPI process. For peroxides such as TATP and HMTD, NR2PI in the DUV region would be one of the best choices. In this approach, excess energy can be minimized by using a tunable laser for observing a molecular ion, the efficiency of which can be drastically improved by using an ultrashort high-peak-power laser. Thus, a tunable femtosecond DUV laser would be desirable for the sensitive as well as the selective detection of these compounds. On the other hand, a RE2PI scheme would be useful for aromatic nitro compounds such as TNT. The ionization efficiency can be improved by means of a resonance effect, and the excess energy should be minimal for the suppression of fragment ions. A femtosecond laser tunable in the DUV region would, therefore, be advantageous for observing a molecular ion. In the case of non-aromatic nitro compounds such as RDX and PENT, it was difficult to observe a molecular ion for RDX and even fragment ions for PENT. These results can be attributed to the fact that the absorption band is located in the VUV region and that the ion easily dissociates to form fragment ions.

In order to further improve the ionization efficiency, the use of a tunable DUV laser with a shorter pulse width and a larger pulse energy would be desirable. Another issue would be the use of a resonance effect. A tunable femtosecond laser emitting in the VUV region could be employed for resonance excitation which could be followed by ionization using a UV - VIS femtosecond laser to minimize excess energy that is produced. Such an approach based on two-color RE2PI, which is especially attractive for non-aromatic nitro compounds such as RDX and PETN, could be achieved using a couple of emission lines generated by the four-wave Raman mixing used in this study.

ACKNOWLEDGMENTS

This research was supported by a Grant-in-Aid for Scientific Research from the Japan Society for the Promotion of Science (JSPS KAKENHI Grant Number 23245017, 24510227, 26220806, 26248037). The quantum chemical calculations were mainly carried out using the computer facilities at the Research Institute for Information Technology, Kyushu University.

REFERENCES

1. Caygill, J. S.; Davis, F.; Higson, S. P. J. *Talanta* **2012**, 88, 14-29.
2. Lubman, D. M. *Anal. Chem.* **1987**, 59, 31A-40A.
3. Weickhardt, C.; Tonies, K. *Rapid Commun. Mass Spectrom.* **2002**, 16, 442-446.
4. Mullen, C.; Irwin, A.; Pond, B. V.; Huestis, D. L.; Coggiola, M. J.; Oser, H. *Anal. Chem.* **2006**, 78, 3807-3814.
5. Yamaguchi, S.; Uchimura, T.; Imasaka, T.; Imasaka, T. *Rapid Commun. Mass Spectrom.* **2009**, 23, 3101-3106.
6. Schramm, E.; Muhlberger, F.; Mitschke, S.; Reichardt, G.; Schulte-Ladbeck, R.; Putz, M.; Zimmermann, R. *Appl. Spectrosc.* **2008**, 62, 238-247.
7. Zhu L.; Johnson, P. J. *Chem. Phys.* **1991**, 94, 5769-5771.
8. Imasaka, T. *Anal. Bioanal. Chem.* **2013**, 405, 6907-6912.
9. Shitamichi, O.; Imasaka, T. *Optics Express* **2012**, 20, 27959-27965.
10. Li, A.; Uchimura, T.; Watanabe-Ezoe, Y.; Imasaka, T. *Anal. Chem.* **2011**, 83, 60-66.
11. Chang, Y. C.; Imasaka, T. *Anal. Chem.* **2013**, 85, 349-354.
12. Cooper, J. K.; Grant, C. D.; Zhang, J. Z. *Reports in Theoretical Chemistry* **2012**, 11, 11-19.
13. Cooper, J. K.; Grant, C. D.; Zhang, J. Z. *J. Phys. Chem. A*, **2013**, 117, 6043-6051.
14. Ezoe, R.; Imasaka, T.; Imasaka, T. *Anal. Chim. Acta*, **2015**, 853, 508-513.
15. Shimizu, T.; Watanabe-Ezoe, Y.; Yamaguchi, S.; Tsukatani, H.; Imasaka, T.; Zaitsev, S.; Uchimura, T.; Imasaka, T. *Anal. Chem.* **2010**, 82, 3441-3444.
16. Mullen, C.; Huestis, D.; Coggiola, M.; Oser, H. *Int. J. Mass Spectrom.* **2006**, 252, 69-72.
17. Oxley, J.; Zhang, J.; Smith, J.; Cioffi, E. *Prop. Explos., Pyrotech.* **2000**, 25, 284-287.
18. McLuckey, S. A.; Glish, G. L.; Kelley, P. E. *Anal. Chem.* **1987**, 59, 1670-1674.
19. McLuckey, S. A.; Glish, G. L. *Org. Mass Spectrom.* **1987**, 22, 224-228.

20. Mullen, C.; Coggiola, M. J.; Oser, H. *J. Am. Soc. Mass Spectrom.* **2009**, *20*, 419-429.
21. Delgado, T.; Alcántara, J. F.; Vadillo, J. M.; Lserna, J. *Rapid Commun. Mass Spectrom.* **2013**, *27*, 1807-1813.
22. National Institute of Standards and Technology (NIST), *NIST Standard Reference Database*, 69 - February 2000 Release: *NIST Chemistry Webbook*, US Secretary of Commerce on Behalf of the United States of America.
23. Harris, N. J.; Lammertsma, K. *J. Am. Chem. Soc.* **1997**, *119*, 6583-6589.
24. Hayashi, R.; Kowhakul, W.; Susa, A.; Koshi, M. *Sci. Technol. Ener. Mater.* **2009**, *70*, 62-67.

Table 1 Relative intensity of the molecular ion peak and the base peak

Method	Relative intensity (%)	Reference
Electron Ionization	0.1	15
VUV Single-photon Ionization	3.5	4
NIR Multi-photon Ionization at 795 nm	9.1	16
DUV Two-photon Ionization at 267 nm		
<u>Pulse Width</u>		
260 fs	1.7	15
200 fs	4.2	5
60 fs	15	15
35 fs	60	14
35 fs*	150	This work

*The pulse was compressed using a pair of prisms.

Figure Captions

Fig. 1 Experimental setup. CM, concave mirror; DM, dielectric multilayer mirror; M, mirror.

Fig. 2 Chromatograms for the explosives. (a) TATP, 267 nm (b) HMTD, 267 nm (c) TNT, 219 nm (d) RDX, 219 nm. The conditions for GC separation are described in detail in the experimental section. Monitoring ion, (a) (b) (c) molecular ion (d) fragment ion ($m/z = 128$). A signal of internal standard (IS) appeared in (a) (b) (c) by an increase in the baseline due to a strong signal of IS.

Fig. 3(a) calculated absorption spectrum for TATP. (b) (c) (d) mass spectra measured at 267, 241, and 219 nm, respectively.

Fig. 4 (a) calculated absorption spectrum for HMTD. (b) (c) (d) mass spectra measured at 267, 241, and 219 nm, respectively. A sharp spike at ca. $m/z = 180$ in (c) is attributed to a noise. Note that the scale of (c) is three times expanded compared to that of (b).

Fig. 5 (a) calculated absorption spectrum for TNT. (b) (c) (d) mass spectra measured at 267, 241 nm and 219 nm, respectively.

Fig. 6 (a) calculated absorption spectrum for RDX. (b) (c) (d) mass spectra measured at 267, 241 , and 219 nm, respectively. No signal peak corresponding to a molecular ion, $[M]^+$, is observed at $m/z = 222$ in the mass spectrum.

Fig. 7 (a) calculated absorption spectrum for PETN.

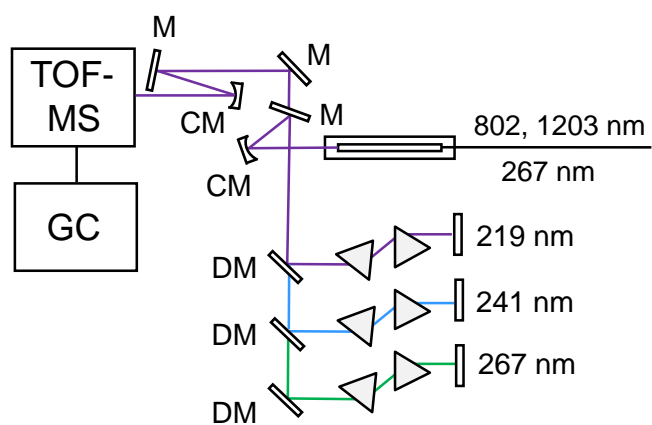


Fig. 1 A. Hamachi et al.

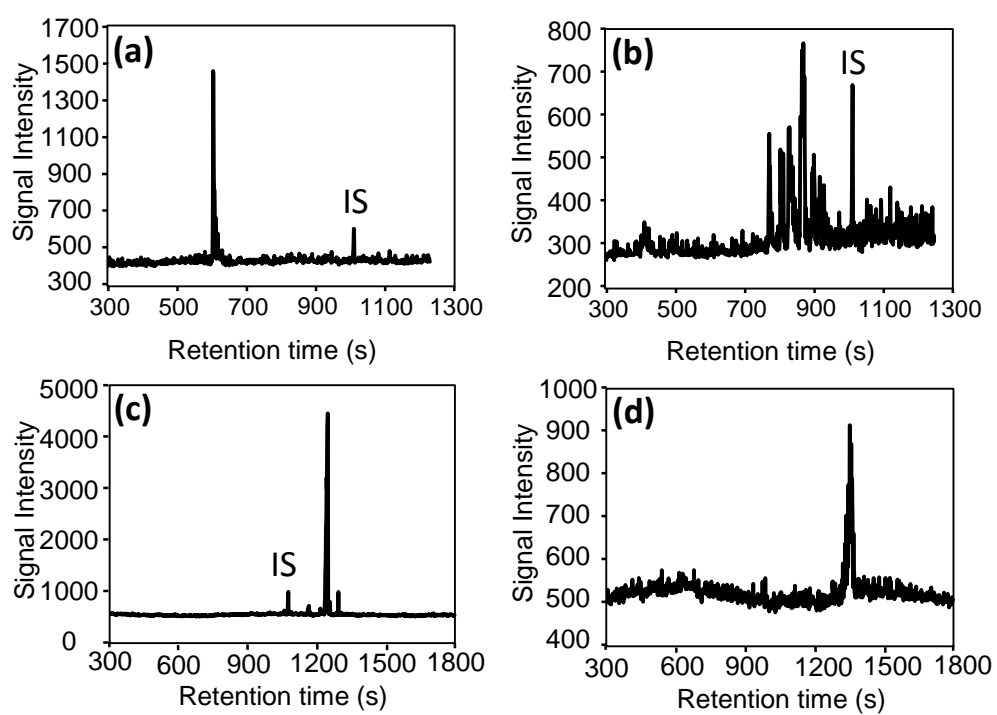


Fig. 2 A. Hamachi et al.

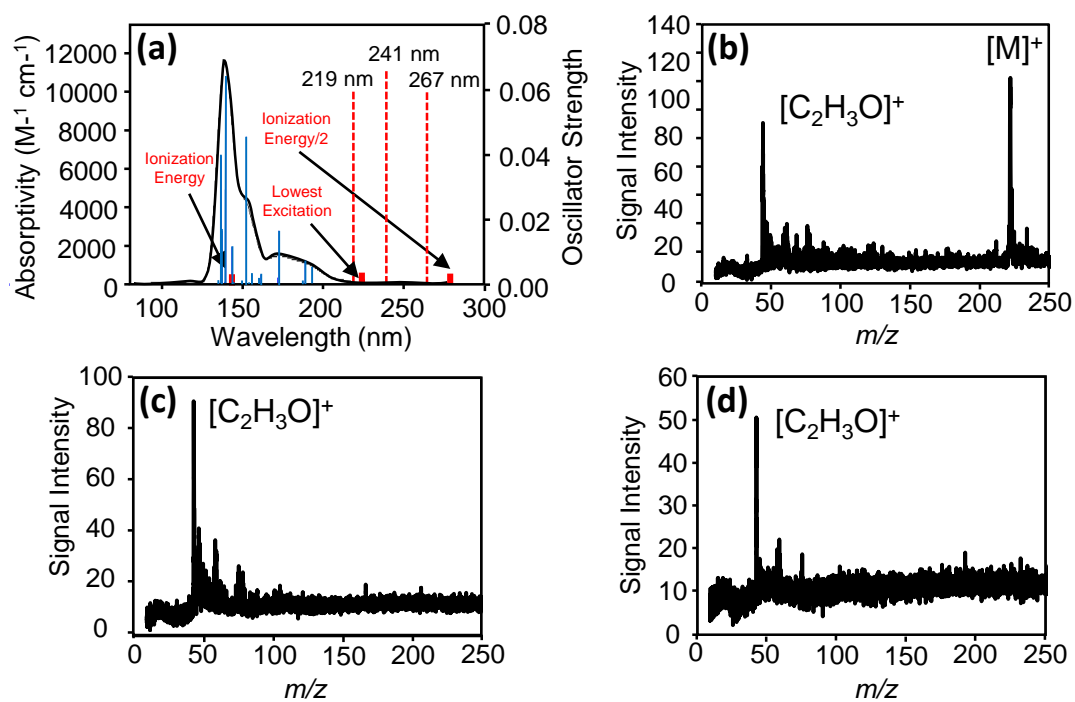


Fig. 3 A. Hamachi et al.

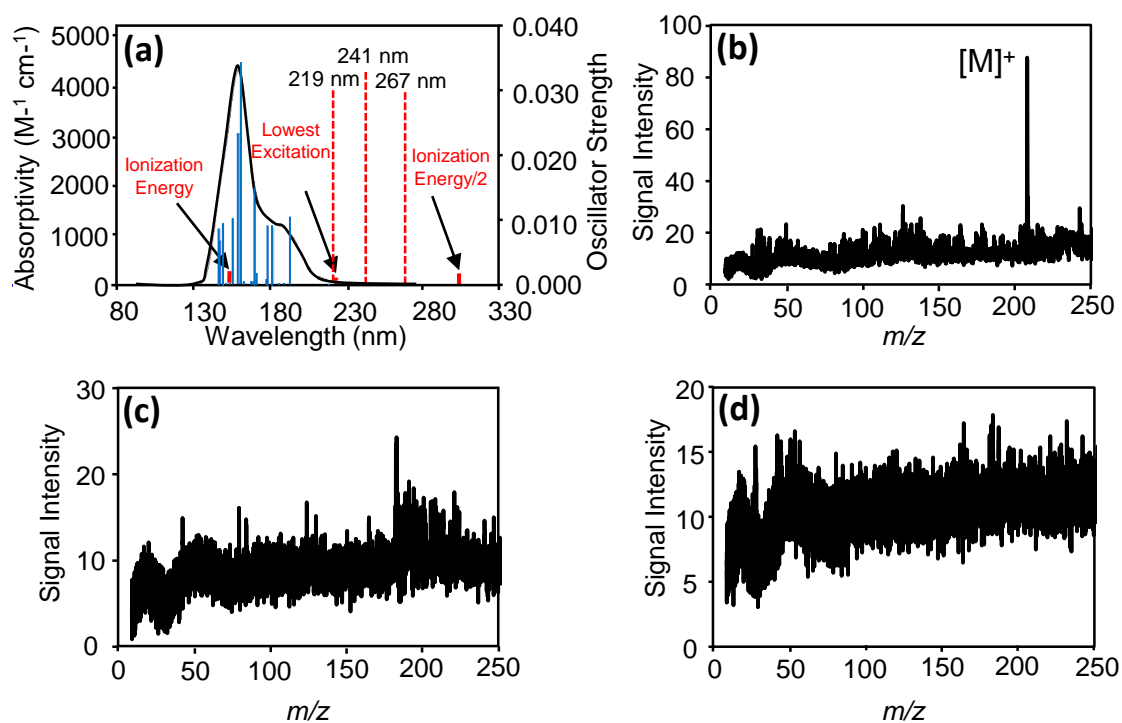


Fig. 4 A. Hamachi et al.

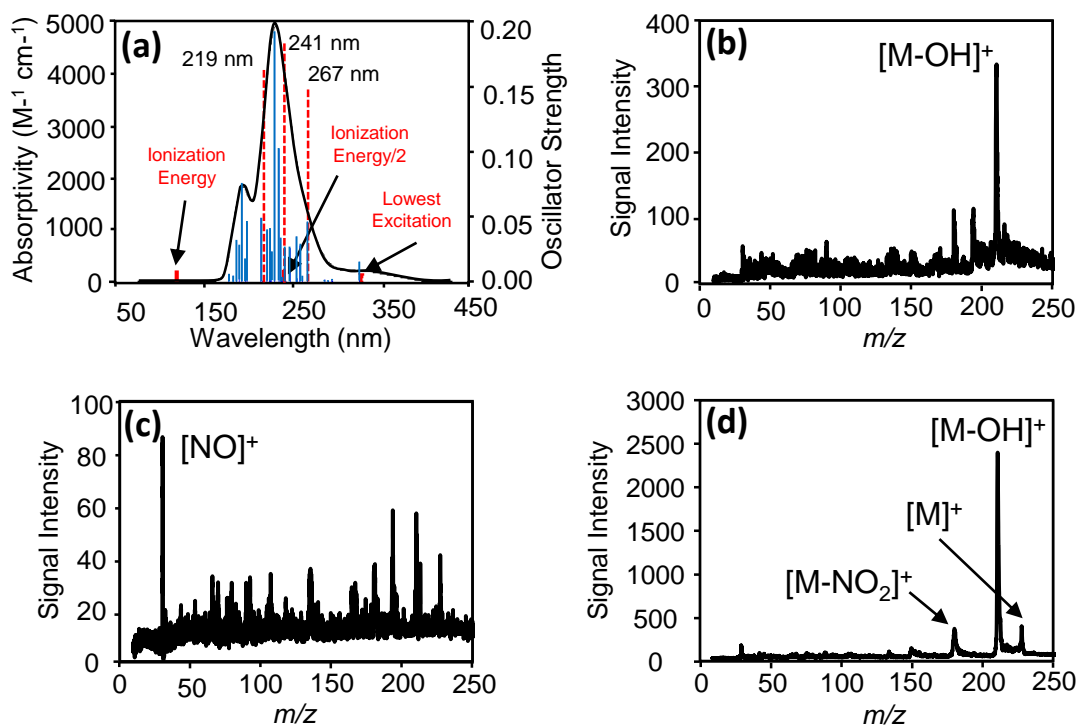


Fig. 5 A. Hamachi et al.

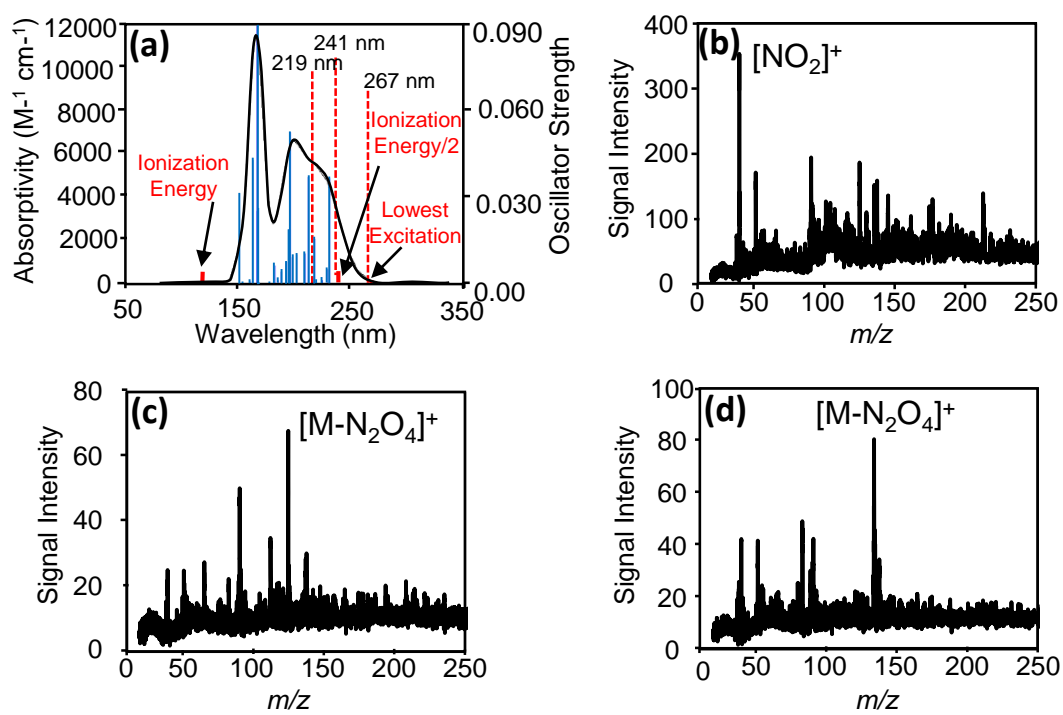


Fig. 6 A. Hamachi et al.

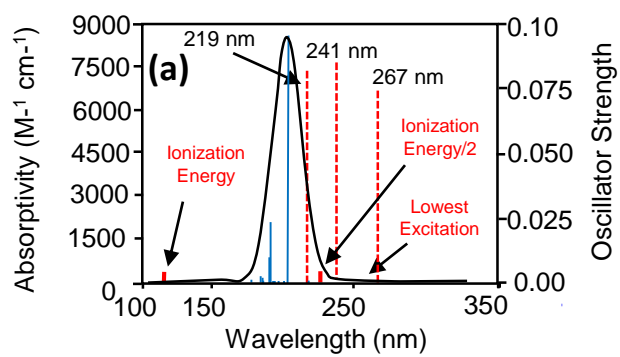


Fig. 7 A. Hamachi et al.